Available online at www.sciencedirect.com

SciVerse ScienceDirect

Acta Materialia 60 (2012) 811–818

Acta MATERIALIA

www.elsevier.com/locate/actamat

Surface topography and energy of grain boundary triple junctions in copper tricrystals

B. Zhao [a,*], A. Ziemons [a], L.S. Shvindlerman [a,b], G. Gottstein [a]

[a] *Institut für Metallkunde und Metallphysik, RWTH Aachen University, Aachen, Germany*
[b] *Institute of Solid State Physics, Russian Academy of Sciences, Chernogolovka, Moscow District, Russia*

Received 17 August 2011; received in revised form 17 October 2011; accepted 17 October 2011
Available online 14 December 2011

Abstract

Copper tricrystals with a common crystallographic axis ⟨100⟩, ⟨110⟩, ⟨111⟩ were fabricated by the Bridgman technique. Utilizing atomic force microscopy, the topography of the grain boundary triple junctions for the three crystallographic systems were investigated. The grain boundary free surface energy and the grain boundary triple line energy were determined for specific crystallographies of tricrystals.

Keywords: Grain boundary triple junction; Grain boundary triple line energy; Grain boundary free surface energy; Tricrystal

1. Introduction

Grain boundary triple junctions affect materials' behavior, especially the microstructural evolution of polycrystalline materials. In particular, they can exert a considerable drag on moving grain boundaries [1–3]. Recent studies have demonstrated that triple junctions have distinct thermodynamic and kinetic properties that distinguish them from the connected grain boundaries. A limited mobility of grain boundary triple lines is one cause of grain boundary drag and slows down grain growth in nanocrystalline materials [4,5]. Grain boundary triple lines, as one structural element of polycrystals, therefore, have been recognized to impact microstructural evolution [6–8]. This generates new opportunities for controlling and designing fine grained and nanocrystalline materials through the impact of triple junction drag on recovery, recrystallization, and grain growth.

While grain boundary thermodynamics and kinetics have been addressed frequently in the past, very little is known of the thermodynamic properties of grain boundary junctions. They have been identified as nucleation sites for precipitation and recrystallization [9], and as a locus of plastic yielding, allowing plastic deformation to occur in both polycrystalline bulk material and thin films [8,10,11]. Also, during creep deformation at high temperatures, triple lines constitute major obstacles to grain boundary sliding and frequently are nucleation sites for cracks [12]. They were also found as the location of enhanced solute segregation of bismuth in copper [13] owing to the line tension of grain boundary triple lines which in turn causes a drag effect of solute atoms on triple junction motion and consequently on triple junction mobility.

These examples demonstrate that grain boundary triple lines have properties distinct from those of the connected grain boundaries. However, so far only a few attempts have been made to investigate the triple line energy experimentally as well as theoretically. Nishimura [14] and Fortier et al. [15] assumed that the triple junction pit on the surface has the shape of a tetrahedron, and on this basis they determined the triple line energy to be at least 5×10^{-7} J m^{-1} in copper. With the same concept, Kim et al. [16] concluded from results on nanocrystalline thin films of ZrO_2 that

* Corresponding author.
E-mail addresses: zhao@imm.rwth-aachen.de, zhaoicyice@googlemail.com (B. Zhao).

1359-6454/$36.00 © 2011 Acta Materialia Inc. Published by Elsevier Ltd. All rights reserved.
doi:10.1016/j.actamat.2011.10.034

~20% of the triple junctions in ZrO_2 exhibited a detectably elevated energy. As shown in Ref. [17], however, the measured quantity did not reflect the true grain boundary triple line energy. It can be determined, though, if the dependence of the grooving angle on groove root curvature is taken into account [17]. Since a curved groove root experiences an additional pressure, similar to the Laplace pressure, it is possible to measure the grain boundary free surface triple line energy, i.e. the energy of the groove root line. For polycrystalline copper it was determined to amount to $(16.8 \pm 7.0) \times 10^{-9}$ J m^{-1} [17]. The grain boundary triple line tension can then be derived from the line tension equilibrium of three grain boundary groove roots and the triple line (Fig. 1). For a random triple line in copper it was measured to be $(6.3 \pm 2.8) \times 10^{-9}$ J m^{-1} [17]. However, all previous results were obtained on random grain boundaries and triple lines. In this work, we used the method outlined in Ref. [17] to derive the grain boundary free surface energy and grain boundary triple line energy in copper tricrystals with defined crystallography.

When a grain boundary is perpendicular to the surface, and the orientation dependency of the surface energy can be neglected, the grain boundary energy can be derived from a measurement of the dihedral angle on a straight groove root (Fig. 2a):

$$\gamma_B = 2\gamma_S \cos\frac{\theta}{2} \tag{1}$$

where θ is the dihedral angle, and γ_S, γ_B are the free surface energy and grain boundary energy, respectively. The dihedral angle θ will be changed by a curvature of the groove root to an angle ξ (Fig. 2b). By measuring the dihedral angles of the groove root with curvature, the grain boundary free surface triple line tension γ^{IS} can be determined:

$$\gamma^{IS} = 2\gamma_S\left(\cos\frac{\theta}{2} - \cos\frac{\xi}{2}\right)\cdot R \tag{2}$$

where R is the radius of curvature at a given point of the groove root.

The force equilibrium in the triple line direction yields the grain boundary triple line energy:

$$\gamma^{l}_{TL} = \gamma^{IS}_{1-2}\sin\zeta_{1-2} + \gamma^{IS}_{1-3}\sin\zeta_{1-3} + \gamma^{IS}_{2-3}\sin\zeta_{2-3} \tag{3}$$

ζ_{1-2}, ζ_{1-3}, and ζ_{2-3} are the inclination angles of each groove root at the triple junction (Fig. 1b).

2. Experimental setup

To obtain crystallographically defined tricrystalline specimens, copper tricrystals with specific orientations of three single crystal seeds were grown by the Bridgman technique [18] in a vacuum of $\sim 10^{-5}$ mbar (Fig. 3). The orientations of the grains in the tricrystals were characterized by the X-ray Laue technique after tricrystal growth, with an accuracy of 0.1°. With the coordinate system given in Fig. 4, the

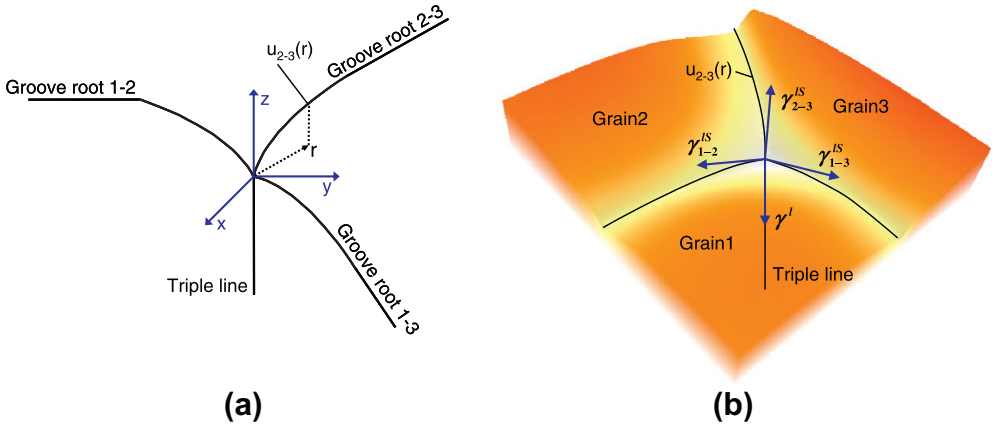

Fig. 1. (a) Schematic three-dimensional (3-D) view of the line geometry at a triple junction. (b) AFM 3-D view of the line tension equilibrium at a triple junction.

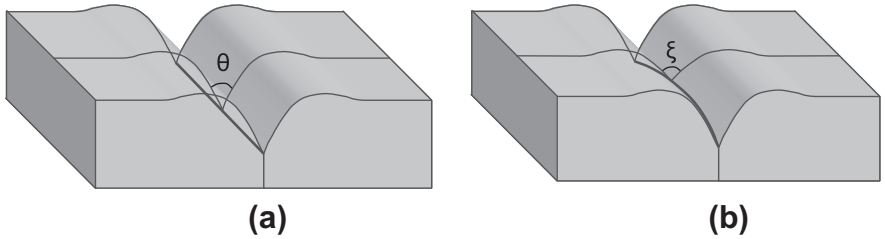

Fig. 2. (a) Grain boundary groove formed at a flat grain boundary with no variation in height. (b) Grain boundary of a flat grain boundary with a curved groove root.

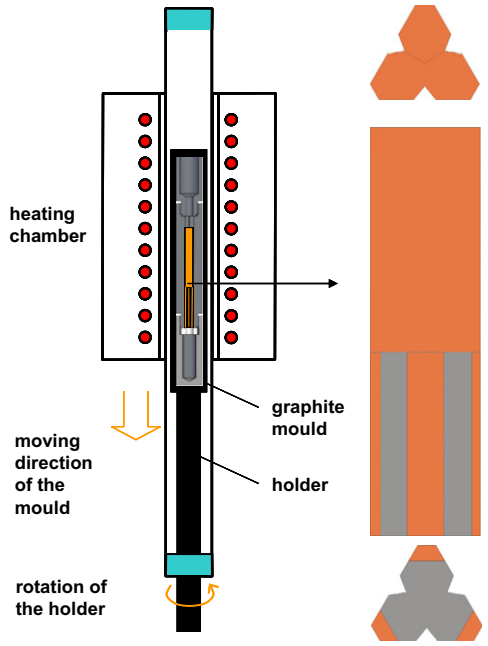

Fig. 3. Schematic arrangement for the tricrystal fabrication in a Bridgman furnace.

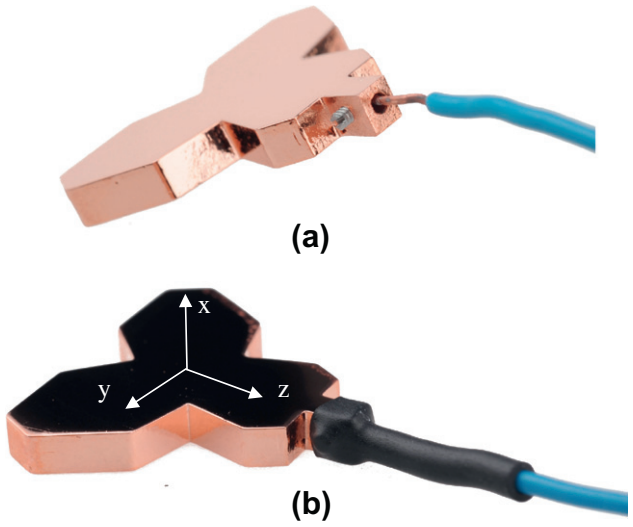

Fig. 4. Tricrystal geometry used for electropolishing: (a) fixing of the wire and (b) protection from contamination.

deviation of the common crystallographic axis from the normal of the specimen (x-axis) will be given by the rotation angles Δy, Δz with respect to the y-axis and z-axis.

A grown tricrystal was sectioned perpendicular to the longitudinal specimen axis into slices of 2 mm thickness. These slices were etched with nitric acid to reveal the location of the grain boundaries on both the top and bottom surface to ascertain that the grain boundaries and triple junctions were perpendicular to the surface. They were ground with abrasive paper P1200, P2400, and P4000 and then mechanically polished with a water-based diamond suspension of 3 μm and 1 μm.

To obtain a smooth surface, electropolishing was used [19]. The specimens were shaped by spark erosion (Fig. 3), and two holes with diameter 1 mm perpendicular to each other were drilled on a lateral surface to connect a copper cable to the specimen. It was fixed by a 1 mm screw driven from the other hole (Fig. 4a). The attachment was hosed by an electrically insulating slip tube which was shrunk by heat for a tight fit to avoid contamination of the electrolyte (Fig. 4b).

The specimens were electropolished at room temperature in a still electrolyte (274 ml 85% ortho-phosphoric acid + 66 ml distilled water). The low voltage of 1.75 V caused a slow electropolishing for at least 1 h, which guaranteed a high surface quality.

After electropolishing, the copper tricrystal specimens were annealed at 980 °C for 2 h in a vacuum furnace. To ensure the formation of a thermal groove by surface diffusion, the specimens were covered with an alumina sheet to reduce evaporation of the surface. Subsequently, the surface topography of the tricrystal was examined by atomic force microscopy (AFM).

The raw data of AFM images consist of a series of discrete points in three dimensions and have to be converted by a specific software to realistic features, e.g. by removing surface tilting, which could introduce an additional error for angle measurements.

The softwares XEI and scanning probe image processor (SPIP) can easily derive the profiles from AFM images. To extract the profile of a groove and the dihedral angle with high precision, we used the raw data of the AFM images after a plane fit. Then, the dihedral angle can be derived from the profile on a plane perpendicular to the surface.

After such fit of the whole area, the deepest point of the profile is associated with the position of the triple junction. Correspondingly, the image is subdivided into three sectors, each of which has one grain boundary. The three sectors are examined line by line. The deepest point of each line corresponds to the groove root. This information is used for further analysis.

3. Results

The misorientations of the three grain boundaries in a ⟨100⟩ copper tricrystal were GB_{12}: 21.3°⟨100⟩, GB_{13}: 30.7°⟨100⟩, GB_{23}: 9.4°⟨100⟩. Fig. 5a and b reveals a top and bottom view of the surface in the vicinity of the ⟨100⟩ triple junction. The measured thermal groove depth, the dihedral angle of the three grain boundaries, the grain boundary energy and the deviations of the ⟨100⟩ axis from the normal of the specimen in each grain are given in Table 1. It is obvious that the low angle grain boundary GB_{23} has the lowest energy, and thus renders a shallow groove root towards the triple junction (Fig. 5b).

The groove root of GB_{23} was observed to be slightly curved (Fig. 6) in the vicinity of the triple junction, and accordingly, this caused a change of the dihedral angle. The curved segments on the 9.4°⟨100⟩ grain boundary had

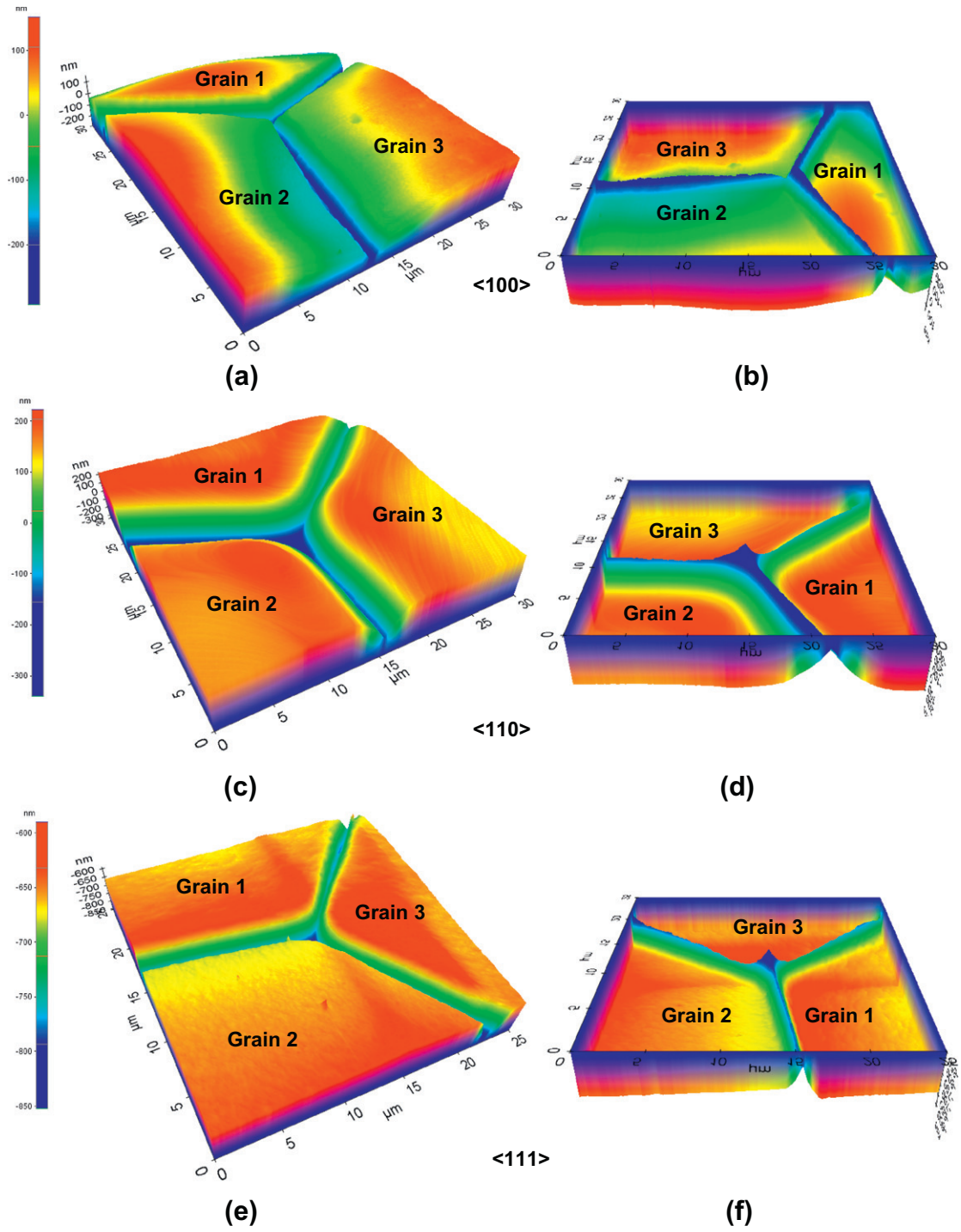

Fig. 5. Top and bottom views of AFM topography measurements in the vicinity of a triple junction. AFM image step size was 0.12 μm. (a and b) are top and bottom views of a ⟨100⟩ tricrystal; (c and d) are top and bottom views of a ⟨110⟩ tricrystal; (e and f) are top and bottom views of a ⟨111⟩ tricrystal.

an average radius of $R_{100} = (260 \pm 97)$ nm, with a dihedral angle $\xi = 164.0° \pm 1.7°$. This corresponds to a grain boundary free surface line tension of $(28 \pm 17) \times 10^{-9}$ J m^{-1}.

The other groove roots were smooth so that the grain boundary free surface line tensions were associated with the previously determined value $(21 \pm 9) \times 10^{-9}$ J m^{-1} [17,20]. The grain boundary triple line energy in the ⟨100⟩ tricrystal was found as $(5.3 \pm 1.9) \times 10^{-9}$ J m^{-1}.

The misorientations of the three grain boundaries in the ⟨110⟩ copper tricrystal were GB_{12}: 38.8°⟨110⟩, GB_{13}: 87.6°⟨110⟩, GB_{23}: 47.7°⟨110⟩. Fig. 5c and d gives the top and bottom view of the surface in the vicinity of the ⟨110⟩ triple junction. The grain boundary thermal grooves had profiles as predicted by the surface diffusion controlled grooving theory [21]. The measured values are listed in Table 2.

Table 1
Data of ⟨100⟩ Tricrystal.

⟨100⟩ tricrystal	Grain 1 $\Delta y = 1.1$ $\Delta z = 1.5$	Grain 2 $\Delta y = 0.9$ $\Delta z = -0.5$	Grain 3 $\Delta y = -0.1$ $\Delta z = -0.2$
Misorientation	GB12: 21.3°⟨100⟩	GB13: 30.7°⟨100⟩	GB23: 9.4°⟨100⟩
α (°)	109.6	111.3	139.1
γ_B/γ_S	0.39 ± 0.03	0.37 ± 0.03	0.22 ± 0.07
Depth (nm)	184	178	80
ζ (°)	2.6 ± 0.9	2.8 ± 1.2	8.1 ± 2.4
γ_{lS} (10^{-9} J m^{-1})	21 ± 9	21 ± 9	28 ± 17
γ_{TL} (10^{-9} J m^{-1})		5.3 ± 1.9	

Table 2
Data of ⟨110⟩ Tricrystal.

⟨110⟩ tricrystal	Grain 1 $\Delta y = -1.5$ $\Delta z = -1.7$	Grain 2 $\Delta y = 1.5$ $\Delta z = 0.9$	Grain 3 $\Delta y = 0.4$ $\Delta z = -0.4$
Misorientation	GB_{12}: 38.8°⟨110⟩	GB_{13}: 87.6°⟨110⟩	GB_{23}: 47.7°⟨110⟩
α (°)	97.5	132.5	130.1
γ_B/γ_S	0.37 ± 0.02	0.24 ± 0.01	0.32 ± 0.01
Depth (nm)	313	212	265
ζ (°)	4.7 ± 0.8	7.9 ± 0.2	3.5 ± 0.8
γ_{lS} (10^{-9} J m^{-1})	21 ± 9	24 ± 15	21 ± 9
γ_{TL} (10^{-9} J m^{-1})		6.3 ± 2.3	

The misorientation of grain boundary GB_{13} was near to $\Sigma = 17$, and thus had a low grain boundary energy. Similar to the low angle grain boundary 9.4°⟨100⟩, small undulations of the groove root were observed near the triple junction, with an average size of $R_{110} = (139 \pm 66)$ nm and a dihedral angle $\xi = 160.9° \pm 2.2°$. Correspondingly, the grain boundary free surface line tension was $(24 \pm 15) \times 10^{-9}$ J m^{-1}. Taking the grain boundary free surface line tension of the other two grain boundaries as $(21 \pm 9) \times 10^{-9}$ J m^{-1}, the corresponding grain boundary triple line tension was $(6.3 \pm 2.3) \times 10^{-9}$ J m^{-1}.

The misorientations of the ⟨111⟩ tricrystal were GB_{12}: 41.0°⟨111⟩, GB_{13}: 58.1°⟨111⟩, GB_{23}: 18.8°⟨111⟩. It comprised neither a low angle grain boundary nor a low Σ grain boundary. The measured values are given in Table 3. The groove roots in the ⟨111⟩ tricrystal were all smoothly curved towards the triple junction (Fig. 5f), and rendered the angle ζ to be 6.5–10°. The grain boundary with the lowest energy had the largest angle ζ. With the average grain boundary free surface line tension $(21 \pm 9) \times 10^{-9}$ J m^{-1}, the grain boundary triple line tension in the ⟨111⟩ tricrystal is $(9.2 \pm 2.7) \times 10^{-9}$ J m^{-1}.

Table 3
Data of ⟨111⟩ Tricrystal.

⟨111⟩ tricrystal	Grain 1 $\Delta y = 0.6$ $\Delta z = 0.1$	Grain 2 $\Delta y = 0.6$ $\Delta z = -1.0$	Grain 3 $\Delta y = 0.2$ $\Delta z = -0.01$
Misorientation	GB_{12}: 41.0°⟨111⟩	GB_{13}: 58.1°⟨111⟩	GB_{23}: 18.8°⟨111⟩
α (°)	115.6	122.2	122.2
γ_B/γ_S	0.39 ± 0.07	0.33 ± 0.02	0.35 ± 0.5
Depth (nm)	309	231	249
ζ (°)	6.5 ± 2.5	10.0 ± 2.4	8.8 ± 2.0
γ_{lS} (10^{-9} J m^{-1})	21 ± 9	21 ± 9	21 ± 9
γ_{TL} (10^{-9} J m^{-1})		9.2 ± 2.7	

4. Discussion

4.1. Force equilibrium at a triple junction

The force equilibrium at a triple junction in the plane perpendicular to the triple line (horizontal plane) is given by

$$\sum_i \left[\gamma_i \vec{t}_i + \left(\frac{\partial \gamma}{\partial \alpha} \right)_i \vec{n}_i + \gamma_i^{lS} \cos \zeta_i \vec{t}_i + \left(\frac{\partial \gamma^{lS} \cos \zeta}{\partial \alpha} \right)_i \vec{n}_i \right] = 0$$

where all the tangential (unit vector $\vec{t}_i$) and normal (unit vector $\vec{n}_i$) forces are taken into account. In the classical model, the equilibrium at a triple junction is determined only by the energy of the attached grain boundaries. If torque terms $\left(\left(\frac{\partial \gamma}{\partial \alpha} \right)_i \vec{n}_i \right)$ are neglected, the relation of the contact angles of three grain boundaries at a triple junction is given by the Young–Dupré equation [22] (Fig. 7a):

$$\frac{\gamma_{B_{12}}}{\sin \alpha_3} = \frac{\gamma_{B_{23}}}{\sin \alpha_1} = \frac{\gamma_{B_{31}}}{\sin \alpha_2}$$

where only the grain boundary energies are taken into account. In a real system with thermal grooves on both surfaces of the specimen, there is an additional term owing to

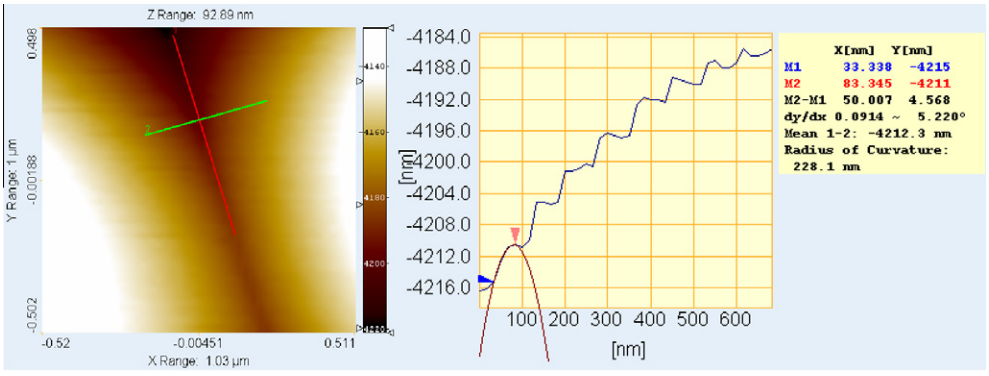

Fig. 6. Groove root profile of a 9.4°⟨100⟩ grain boundary.

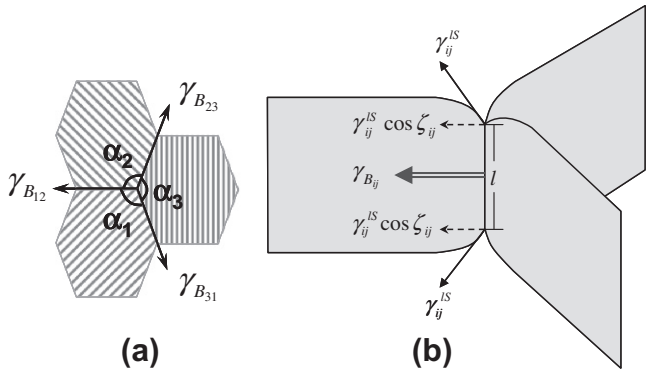

Fig. 7. (a) Equilibrium of grain boundary surface tensions in the horizontal plane. (b) Force component of the groove root with tangential angle ζ.

the contribution of the grain boundary free surface line tension in the horizontal plane (Fig. 7b). When the grain boundary free surface line tension is taken into account for the equilibrium at the triple junctions and all torque terms are neglected, the Young–Dupré equation is modified to

$$\frac{\gamma_{B_{12}}\cdot l+2\gamma_{12}^{IS}\cos\zeta_{12}}{\sin\alpha_3}=\frac{\gamma_{B_{23}}\cdot l+2\gamma_{23}^{IS}\cos\zeta_{23}}{\sin\alpha_1}=\frac{\gamma_{B_{31}}\cdot l+2\gamma_{31}^{IS}\cos\zeta_{31}}{\sin\alpha_2}$$

under the assumption that the triple line is straight and perpendicular to the horizontal plane; l is the length of the triple line, and the factor 2 is due to thermal grooves on both surfaces of the sample (Fig. 7b).

In our case, the specimens had a thickness of 2 mm, hence the equilibrium of the grain boundaries at the triple junction was essentially determined by the grain boundary energies only, and the contribution of the three groove root line tensions was negligible. For example, the grain boundaries in the $\langle 1\,1\,1\rangle$ tricrystal were all random high angle grain boundaries. Therefore, we can assume the same grain boundary energy for all three grain boundaries, and torque terms can be neglected. The sum of forces of the three groove root line tensions at the triple junction in the horizontal plane was just 1×10^{-9} J m^{-1} in the direction opposite grain boundary GB_{12}, and the contact angles α_i differed by only 5% from the values predicted by Eq. (6). Hence, within the range of experimental error the measurements complied with Eqs. (4) and (6), respectively. However, for a Cu film with a thickness $\leqslant$70 nm, the effect of the grain boundary free surface line tension becomes comparable to the grain boundary energy and has to be taken into account for the force equilibrium at the junction.

4.2. Dependence of triple line tension on crystallography

Due to the different misorientations of the grain boundaries, the grain boundary energy varies as reflected by a wide distribution of the groove dihedral angle. Random high angle grain boundaries have larger energies ($\gamma_B/\gamma_S\approx0.35$) than low angle grain boundaries, e.g. 9.4°$\langle 1\,0\,0\rangle$, and special grain boundaries, e.g. 87.6°$\langle 1\,1\,0\rangle$ (near $\Sigma=17$), ($\gamma_B/\gamma_S\approx0.23$).

With a surface energy of 1.75 J m^{-2}, the ratio of the grain boundary energy to the free surface energy is 0.24 ± 0.01 for the 87.6°$\langle 1\,1\,1\rangle$ boundary in qualitative agreement with Ref. [23], where a ratio γ_B/γ_S of 0.26 ± 0.01 was reported for a $\Sigma=11$ grain boundary in copper at 1030 °C.

It was found in our experiments that the specific orientations of the tricrystals engendered a different topography near the triple junctions. Since a thermal groove forms by surface diffusion, the low diffusion coefficient on the $\langle 1\,0\,0\rangle$ surface renders shallow thermal grooves of the $\langle 1\,0\,0\rangle$ grain boundaries. The small undulations (Fig. 6) of the groove root of low energy grain boundaries might have resulted from the interaction of the free surface with the grain boundary to establish the minimum energy state, similar to facets on grain boundaries due to the inclination. The ratio $\frac{\gamma^{IS}}{\gamma_B}$ of the low energy grain boundaries was ~70 nm and comparable to the size of the undulations of the groove root, whereas the ratio $\frac{\gamma^{IS}}{\gamma_B}$ of the random high angle grain boundaries was less than 40 nm. Therefore, the effect of the grain boundary free surface line tension was more obvious on the grain boundaries with low energy, and rendered undulations on the groove root.

At the triple junction, the groove angle ζ reflects the equilibrium of the four competing line tensions. When the energies of the three grain boundaries are comparable, like in the $\langle 1\,1\,1\rangle$ tricrystal, the three groove root triple line tensions are similar. However, when one grain boundary has a lower energy, e.g. GB_{23}: 9.4°$\langle 1\,0\,0\rangle$ in the $\langle 1\,0\,0\rangle$ tricrystal or GB_{13}: 87.6°$\langle 1\,1\,0\rangle$ in the $\langle 1\,1\,0\rangle$ tricrystal, the angle ζ of the other two grain boundaries becomes apparently small and results in a lower triple line energy. We attribute this result to the geometry of the triple line structure, as explained below.

4.3. Interpretation of the orientation dependence of triple line tension

After the heat treatment, the grain boundaries in the tricrystal were in thermodynamic equilibrium, i.e. the atoms in the grain boundaries would possess the same chemical potential. Grain boundaries have a finite width, which can change with temperature [24,25]. The core of intersection of three grain boundaries constitutes the triple line. If we assume the grain boundary energy to increase with its width, i.e. constant grain boundary energy density, the triple line core of intersection will increase with the energy of the adjoining grain boundaries (Fig. 8). In the case where the three grain boundaries have the same energy, the unrelaxed triple line core is an equilateral triangle (Fig. 8a). However, when one grain boundary has a lower energy, the intersection triangle is reduced, and correspondingly the triple line energy is decreased.

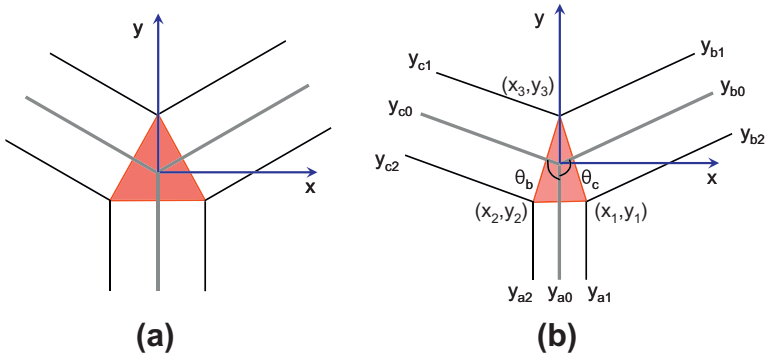

Fig. 8. Schematic view of the intersection of grain boundaries with a certain width. (a) Three grain boundaries with the same energy. (b) One grain boundary possesses a lower energy.

The origin of the coordinate system is associated with the triple junction center. If one grain boundary with the width $2a$ is parallel to the y-axis, then the intersection core can be calculated from the triangle geometry.

The measured ratio of the triple line tension of the $\langle 1\,0\,0\rangle$ and $\langle 1\,1\,0\rangle$ tricrystals to the triple line tension of the $\langle 1\,1\,1\rangle$ tricrystal was 0.57 and 0.67, respectively. The measured grain boundary energies and dihedral angles yielded a triple junction core ratio of 0.68. Although our simple model considers only an unrelaxed grain boundary intersection triangle as a triple line core with constant energy density, it successfully accounts for the measurements. In essence, when there is just one grain boundary with low energy, the triple line energy tends be at least 30% lower than the energy of a general triple line, i.e. that with random crystallography. Our assumption of a constant grain boundary and triple line energy density is, of course, a simplification since a relaxed grain boundary structure may change the energy density. However, especially at high temperatures the structure of the grain boundary is bound to lose any long-range order [26]. From a physical point of view, extremely low triple line energies may be realized for special tricrystal configurations, in analogy to the concept of CSL grain boundaries. This might be one reason why the measured triple line energy in the $\langle 1\,0\,0\rangle$ tricrystal is smaller than predicted by the model.

5. Summary

The topography and energy of grain boundary triple junctions were studied in specific copper tricrystals, which were fabricated by the Bridgman technique. It was found that the surface topography strongly depends on the crystallography of the tricrystal, in particular on the common crystallographic axis of the tricrystal.

The grain boundary free surface line tension, i.e. the line tension of the groove root, for a $9.4°\langle 1\,0\,0\rangle$ grain boundary and $87.6°\langle 1\,1\,0\rangle$ grain boundary, was derived to be $\sim 25\times 10^{-9}\,\mathrm{J\,m^{-1}}$. The grain boundary triple line energy was investigated in $\langle 1\,0\,0\rangle$, $\langle 1\,1\,0\rangle$ and $\langle 1\,1\,1\rangle$ tricrystals, and rendered a triple line energy of $5.3\times 10^{-9}\,\mathrm{J\,m^{-1}} \leqslant \gamma_{TL} \leqslant 9.2\times 10^{-9}\,\mathrm{J\,m^{-1}}$. It was found that the grain boundary triple line energy was lower, if one of the adjoining grain boundaries had a lower energy than the other two. A simple geometrical model was introduced to account for the measured dependency.

Acknowledgements

Financial support of the Deutsche Forschungsgemeinschaft (DFG) through Project Go335/35-2 is gratefully acknowledged. We appreciate the financial support of our cooperation through DFG Grant RUS113/846/0-2(R) and the Russian Foundation of Fundamental Research (Grant DFG-RRFI 09-02-91339).

References

[1] Czubayko U, Sursaeva VG, Gottstein G, Shvindlerman LS. Acta Mater 1998;46:5863.
[2] Upmanyu M, Srolovitz DJ, Shvindlerman LS, Gottstein G. Interface Sci 1999;7:307.
[3] Upmanyu M, Srolovitz DJ, Shvindlerman LS, Gottstein G. Acta Mater 2002;50:1405.
[4] Gottstein G, King AH, Shvindlerman LS. Acta Mater 2000;48:397.
[5] Shvindlerman LS, Gottstein G. Z Metallk 2004;95:239.
[6] Gottstein G, Shvindlerman LS. Z Metallk 2004;95:219.
[7] Gottstein G, Shvindlerman LS. Scripta Mater 2005;52:863.
[8] King AH. Scripta Mater 2010;62:889.
[9] Lefevre-Schlick F, Brechet Y, Zurob HS, Purdy G, Embury D. Mater Sci Eng A 2009;502:70.
[10] Was GS, Thaveeprungsriporn V, Crawford DC. JOM J Miner Met Mater Soc 1998;50:44.
[11] Owusu-Boahen K, King AH. Acta Mater 2001;49:237.
[12] Morris DG, Harries DR. J Mater Sci 1977;12:1587.
[13] Yin KM, King AH, Hsieh TE, Chen FR, Kai JJ, Chang L. Microsc Microanal 1997;3:417.
[14] Nishimura G. MSc thesis. University of Toronto; 1973.
[15] Fortier F, Palumbo GS, Bruce GD, Miller WA, Aust AT. Scripta Metall 1991;25:177.
[16] Kim H, Xuan Y, Ye PD, Narayanan R, King AH. Acta Mater 2009;57:662.
[17] Zhao B, Verhasselt JC, Shvindlerman LS, Gottstein G. Acta Mater 2010;58:5646.
[18] Bridgman PW. In: Proc of the American Academy of Arts and Sciences. Boston: The Academy; 1925. p. 305.

[19] Verhasselt J. Doctoral thesis. RWTH-Aachen University; 2001.
[20] Zhao B, Gottstein G, Shvindlerman LS. Acta Mater 2011;59:3510.
[21] Mullins WW. J Appl Phys 1957;28:333.
[22] Gottstein G. Physical foundations of materials science. Berlin: Springer; 2004. p. 106.
[23] Mclean M. J Mater Sci 1973;8:571.
[24] Keblinsk P, Wolf D, Phillpot SR, Gleiter H. Philos Mag A 1999;79:2735.
[25] Yoon BK, Choi SY, Yamamoto Y, Ikuhara Y, Kang SL. Acta Mater 2009;57:2128.
[26] Wolf W, Yamakov V, Philpot SR, Mukherjee A, Gleiter H. Acta Mater 2005;53:1.